ACS APPLIED POLYMER MATERIALS

pubs.acs.org/acsapm

Article

Hierarchically Porous, Superhydrophobic PLLA/Copper Composite Fibrous Membranes for Air Filtration

Qinghong Huang,[#] Chen Meng,[#] Mingrui Liao, Tianyu Kou, Fangchao Zhou, Jian R Lu, Jiashen Li,[*] and Yi Li[*]

Cite This: *ACS Appl. Polym. Mater.* 2024, 6, 2381−2391

Read Online

ACCESS | Metrics & More | Article Recommendations | Supporting Information

ABSTRACT: Epidemics such as pulmonary tuberculosis and pertussis can spread quickly through the air in enclosed or small spaces. Most of these diseases are caused by various bacteria. In hospitals, nursing homes, and biology laboratories, the requirement for air quality is often high. Particulate air filters can remove infectious bacteria from the air, making them a good choice for local ventilation systems to capture and remove bacteria or other pathogenic microbes. With high surface area, electrospun poly(L-lactic acid) (PLLA) fibrous membranes have the ability to capture small particles like bacteria. Moreover, copper has significant antimicrobial properties. In this Letter, we present a hierarchically porous PLLA membrane created through electrospinning and acetone treatment. Additionally, we describe two methods for loading copper particles onto the hierarchically porous PLLA membrane, thereby providing capabilities for capturing and killing bacteria. The experiments demonstrated that the final PLLA/Cu composite fibrous membranes exhibit not only excellent air permeability but also remarkable antimicrobial performance while maintaining bendability and superhydrophobic ability. This study provides a simple process, low energy cost, and environmentally friendly method to produce the copper-coated PLLA membrane, which is especially suitable for potential applications in high-flux filtration equipment in hospitals, nursing homes, and biology laboratories.

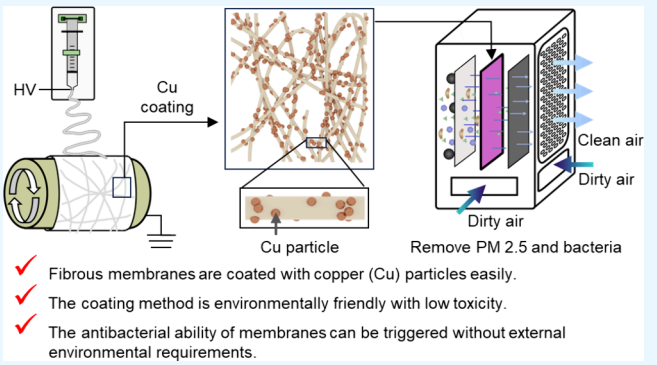

KEYWORDS: *poly(L-lactic acid), electrospinning, nonwoven textiles, antimicrobial copper, air filter*

1. INTRODUCTION

Recently, air pollution caused by fine particulate matter has become one of the most serious environmental concerns in the world.[1−5] The fine particle pollutants in the air, especially particles with an aerodynamic diameter smaller than 2.5 μm (PM2.5), have been shown to be the main causes of cancer, fibrosis, and chronic lung disease.[6] In addition, fine particulate pollutants in the atmosphere also contain various microorganisms, such as *Streptococcus pyogenes*, *Mycobacterium tuberculosis*, and *Bordetella pertussis*, increasing the risk level of air-borne infections.[7,8] In the past, research on the individual protection in outdoor spaces has attracted much attention, such as the design of face mask.[9] However, more studies must also be undertaken to understand how to protect us in enclosed small spaces, such as research laboratories and hospitals.[10,11] These areas require highly efficient filtration tools to keep air clean during the circulation process. An antibacterial filter could serve as a core module in air filter devices[12] and could be potentially used in residential housing, hospital infection control, and biosafety level 3 and 4 laboratories.[13−15] The importance of air filters was further highlighted during the Covid-19 pandemic.[16] Figure 1a,b shows an example of the air purifier usage.

So far, there are two main types of filtration methods that have been extensively studied: porous filters and fibrous filters.[17,18] Compared with porous filters, fibrous filters offer several advantages, e.g., they are easy to mass produce, cost-effective, and energy-efficient. During filtration, big particles are directly blocked by the small gaps among the fibers. Tiny-sized particles, such as viruses, move dramatically slow due to the Brownian diffusion, making them easier to be captured by the fibers.[19] However, due to the large fiber diameter (ranging from a few micrometers to tens of micrometers), traditional fibrous filters—including spun-bonded fibers, glass fibers, and melt-blown fibers—suffer from several shortcomings, such as a low quality factor and a weak ability to capture fine particles.[17]

Received: December 14, 2023
Revised: January 31, 2024
Accepted: January 31, 2024
Published: February 9, 2024

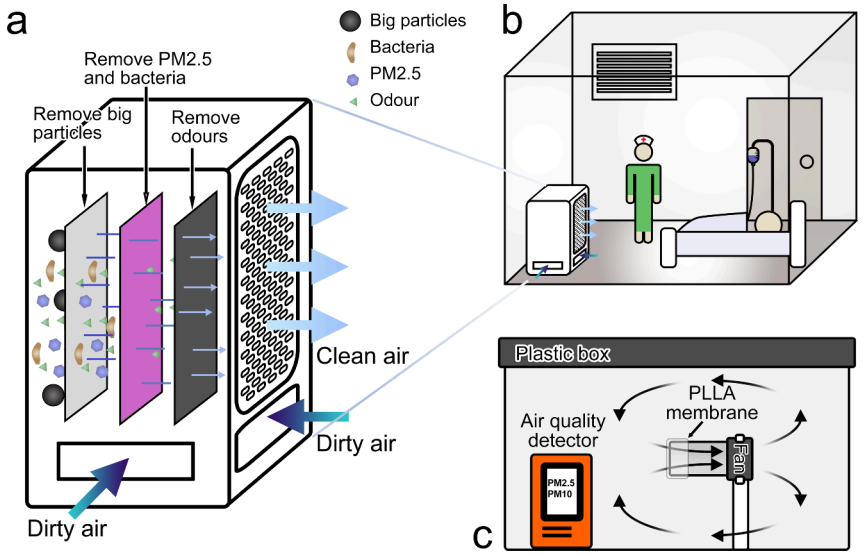

Figure 1. (a) Structure of the air purifier. (b) Usage of air purifier in the hospital. (c) Schematic diagrams of air filtration tests.

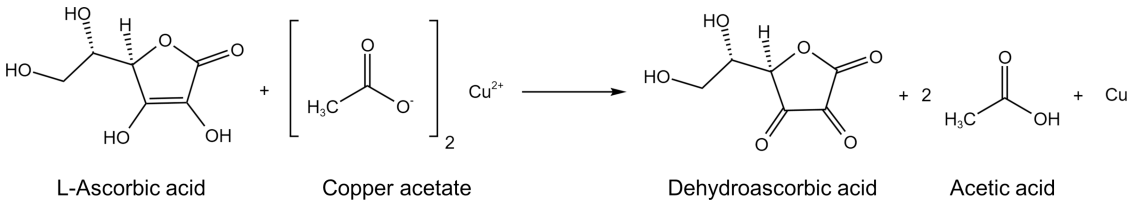

Figure 2. Chemical reaction to make copper nano/microparticles.

Compared with traditional fibrous filters, a piece of electrospun fibrous membrane is composed of micro/nanosized fibers, making it an ideal choice for fibrous filtering.[20,21] Various polymers have been selected and successfully used to fabricate nanofibrous membranes for air filtration such as polyimide, polyacrylonitrile, and polystyrene.[11,22−24] Although electrospun fibrous membranes are effective at capturing PM2.5 and viruses while maintaining air permeability, they still have some inevitable drawbacks, such as relatively low specific surface area and rough surfaces.[25,26]

To endow further antimicrobial properties to filters, some organic compounds were grafted/coated on polymeric fiber membranes[27,28]: Liu et al. electrospun PLLA with tea polyphenol, and the membrane had good tensile strength. However, the membrane's water contact angle was smaller than 90°, and its antimicrobial abilities against both *Escherichia coli* and *Staphylococcus aureus* were less than 99%. Compared with organic compounds, inorganic materials and their compounds, such as silver, copper, and other metallic oxides, offer better stability, stronger attraction to bacterial cell walls, and greater safety.[29,30] The photocatalytic antibacterial ability of TiO_2 is also a hot topic.[31] Choi et al. coated aluminum onto polyester nonwoven air filter, which could capture 99.99% *E. coli* and *Staphylococcus epidermidis*, but it required electrostatic attraction to capture the bacteria.[32] Karthick et al. incorporated silver nanoparticles into an electrospun polyacrylonitrile fibrous membrane-based air filter, resulting in enhanced antimicrobial ability.[33] Comparatively, copper is much more cost-effective than silver and poses fewer biohazards.[34,35] Cu^{2+} can inhibit bacterial growth through the production of intracellular reactive oxygen species (ROS) and can denature bacterial DNA.[35,36] Other than the intracellular antimicrobial mechanisms and physical membrane disruption, the release of nanosized metal oxide in the form of soluble ions has been postulated to be a significant mechanism of action.[37,38] Furthermore, the generation of ROS has been observed to correlate with the crystalline nature of nanometal oxides.[39] These mechanisms may not operate in isolation; rather, it is plausible that multiple factors concurrently contribute to antimicrobial action, suggesting a cooperative mechanism. In addition, copper has good antimicrobial ability and is widely used for the provision of textile products with antimicrobial ability.[40,41] In view of this, copper could be used to prepare a superhydrophobic fibrous membrane with excellent antimicrobial properties.

In this study, acetone treatment was used to create a hierarchically porous PLLA membrane with ultrahigh surface area. This approach nondestructively and effectively enhanced the porosity of the PLLA fibers of the membrane.[42,43] Copper nano/microparticles were loaded on PLLA fiber using copper acetate and L-ascorbic acid at room temperature.[30] The chemical reaction is shown in Figure 2.

Compared with the chemical reagents chosen in other studies, such as the utilization of copper sulfate pentahydrate and borane dimethylamine complex, the coproducts in this study are dehydroascorbic acid and acetic acid, which are environmentally friendly with low toxicity.[44−46] After Cu nano/microparticles were deposited on the PLLA fibrous membrane surface, they were distributed evenly on both sides of the PLLA membrane. The final PLLA/Cu fibrous membrane presented a good antimicrobial ability, excellent air permeability, and superhydrophobicity.

https://doi.org/10.1021/acsapm.3c03055
ACS Appl. Polym. Mater. 2024, 6, 2381−2391

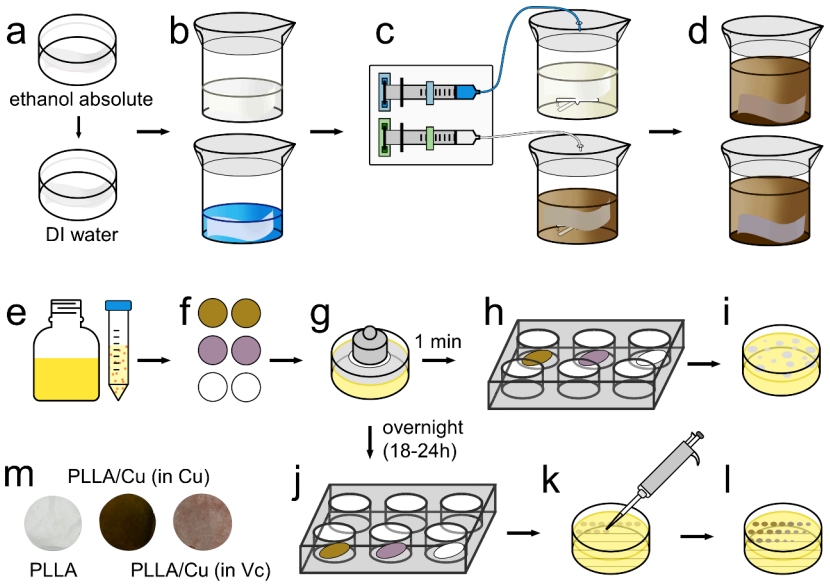

Figure 3. (a–d) Cu particle coating procedure: (a) Membrane samples are immersed in absolute ethanol at first and then transferred to DI water when membranes are still damped. (b) Membrane samples are immersed in an L-ascorbic acid solution/copper acetate solution. (c) The syringe pump is used to add the L-ascorbic acid solution into the copper solution and add the copper solution into the L-ascorbic acid solution. (d) Membranes are set in the solution for about 30 min under closed condition. (e–l) Antibacterial testing procedure: (e) Agar solution (left) and bacterial solution.[51] (f) Thirty-eight millimiter-diameter disc samples of different kinds of membranes. (g) Each membrane sample is placed onto one agar plate, and a cylinder is used to weigh it down for 60 ± 5 s. (h) The disc sample is immersed into a 12 mL PBS solution for 30 min. (i) One hundred microliters of liquid is taken from the solution of each sample and diluted. Then, 10 μL diluted liquid is spread onto one agar plate and incubated. (j) After overnight incubation, another sample of each kind of membrane is immersed into a 12 mL PBS solution for 30 min. (k) A 10 μL solution of the original gradient and each dilution gradient (from 10 to 1 million times) is dipped onto the agar plates. (l) The dipped agar plated is incubated. (m) Picture of disc samples of PLLA, PLLA/Cu (in Cu), and PLLA/Cu (in Vc).

2. EXPERIMENT

2.1. Materials. Dimethylformamide (DMF, 99.80%), copper acetate monohydrate, and L-ascorbic acid (Vc) were bought from Fisher Scientific UK Ltd. PLLA ($M_w \approx 1.43 \times 10^6$) was obtained from PURAC Biomaterials, The Netherlands. Acetone (99.70%) and dichloromethane (DCM) (99.80%) were purchased from Merck Life Science. Ethanol was purchased from VWR international. Gram-negative *E. coli* (ATCC 25922) and Gram-positive *S. aureus* (ATCC 6538) were selected from the American Type Culture Collection (ATCC).

2.2. Sample Preparation. *2.2.1. Fabrication of the Hierarchically Porous PLLA Fibrous Membrane.* Hierarchically porous PLLA fibrous membranes were prepared using a protocol published previously.[42,43] Generally, PLLA granules were added into DCM and stirred until all of the granules were completely dissolved. Then, DMF was added to the solution, and the mixture was stirred for an additional 2 h. The ratio of PLLA to solvents was 1.8:98.2, and the ratio between the two solvents (DCM/DMF) was 95/5. The solution was then transferred to an injection syringe. The syringe was connected to an electrospinning machine (Tongli Tech TL-Pro, China) at 20 kV. The PLLA fibrous membrane was collected and dried in a fume hood for 24 h. For post-treatment, the as-spun PLLA fibrous membrane was immersed in acetone for 5 min at room temperature and then dried in a fume hood. Finally, the prepared hierarchically porous PLLA fibrous membrane was stored appropriately for further use.

2.2.2. Coating the Copper Nanoparticles on the Fibrous Membrane. The coating procedure is illustrated in Figure 3a–d. Initially, the hierarchically porous PLLA fibrous membrane was cut into 8 cm × 8 cm samples. These samples were first wetted with ethanol and then washed with DI water for 3 times. A 25 g/mL L-ascorbic acid solution and 5 g/mL copper acetate solution were prepared by dissolving the reagents in DI water. All samples were divided into 2 groups and transferred into 150 mL of L-ascorbic acid solution and 150 mL of copper acetate solution, respectively, and soaked for approximately 30 min at room temperature in a closed condition. Meanwhile, an additional 150 mL ascorbic acid solution and copper acetate solution were prepared again and loaded into two different syringes. Subsequently, the L-ascorbic acid solution and copper acetate solution were added to the samples using syringe pumps at an injection speed of 90 mL/h. The L-ascorbic acid solution was added to the copper solution, and conversely, the copper solution was added to the L-ascorbic acid solution, as shown in Figure 3c. A magnetic stirrer was used to stir the solution during the reaction.

Once all of the solutions had been added, the membranes were left to soak for an additional 30 min in a closed condition, as shown in Figure 3d. After the reaction was completed, samples were collected and rinsed one time with the ethanol and twice with DI water. The untreated hierarchically porous PLLA fibrous membrane samples were named "PLLA", the membrane samples soaked in L-ascorbic acid solution were named "PLLA/Cu (in Vc)", and the membrane samples soaked in copper acetate were named "PLLA/Cu (in Cu)".

2.3. Characterizations. The surface morphologies of all samples were observed using scanning electron microscopy (SEM, Zeiss Ultra 55). Their elemental composition and distribution were characterized by energy-dispersive spectroscopy (EDS, FEI Quanta 650). X-ray diffraction (XRD) patterns of all samples were detected using an X-ray diffractometer (Philips X'pert XRD5). The mechanical proper-

https://doi.org/10.1021/acsapm.3c03055
ACS Appl. Polym. Mater. 2024, 6, 2381−2391

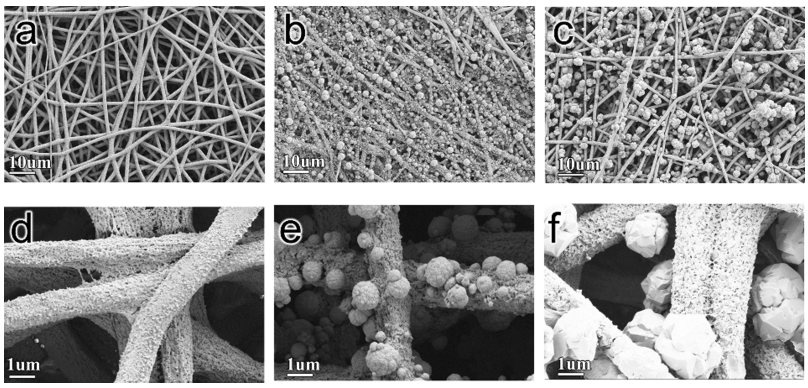

Figure 4. SEM images of (a) PLLA (low magnification), (b) PLLA/Cu (in Cu) (low magnification), (c) PLLA/Cu (in Vc) (low magnification), (d) PLLA (high magnification), (e) PLLA/Cu (in Cu) (high magnification), and (f) PLLA/Cu (in Vc) (high magnification).

ties of the samples were measured by an Instron 3344L3927. Samples were cut into a 5 mm × 25 mm rectangular shape and tested at 5 mm/min extension rate. The water contact angle was tested by a Drop Shape Analyzer (KRUSS, DSA 100). X-ray photoelectron spectroscopy (XPS) was performed with a Kratos Axis (Kratos Analytical Limited), utilizing monochromatized Al Kα radiation. The spot size of the X-ray was around 700 × 300 μm. The thermal behavior was evaluated through thermogravimetric analysis (TGA) using a TGA Q-500 (TA Instruments). Weighed samples were placed into the TGA machine and ramped from room temperature to 500 °C at 10 °C/min in a N_2 atmosphere. The air permeability of the samples was measured by using an air permeability tester (SDL Atlas M021A). The size of the samples was 9 × 9 cm, and the pressure settings used were 50, 100, 150, and 200 Pa.

2.3.1. Air Filtration Experiment. The air filtration ability of the samples was measured using a self-designed combined system, as shown in Figure 1c; an optical image of the system is shown in Figure S1. This system included an air quality detector, a 100 L storage box, an electric fan, and a round holder. Moxa, a traditional Chinese medicine, was used to generate smoke in this experiment, as it contains inhalable particles, carbon monoxide, carbon dioxide, and volatile organic compounds.[47] During the experiment, a Moxa stick was first ignited inside the sealed storage box to generate PM2.5 and PM10 particles. Driven by the electric fan, air flowed continuously through the filter membrane, enabling the capture of the particles in the sealed box. The concentration of PM2.5 and PM10 was recorded by a video camera. After each experiment, the sealed storage box was cleaned with ethanol and left in a fume hood for 12 h to ensure that the air quality inside the box returned to a normal level.

2.3.2. Antibacterial Experiment. The antibacterial test conducted in this study refers to the International Standard BS EN ISO 20743 (2021). The corresponding procedure is shown in Figure 3e–l. Bacteria were inoculated in Mueller–Hinton broth (MHB) overnight and then diluted in MHB to a concentration of approximately 1 × 10^8 CFU/mL for subsequent experiments. Various PLLA membrane discs, each with a diameter of 38 mm, were sterilized under UV light for 30 min and then placed in sterilized Petri dishes. Figure 3m displays the disc samples of PLLA, PLLA/Cu (in Cu), and PLLA/Cu (in Vc).

For the short-time contact antibacterial experiment, a 10 μL bacterial solution was evenly spread across each agar plate. A single disc from each sample type was then placed onto its respective agar plate and weighed down for 60 ± 5 s using a 200 g stainless-steel weight. After that, the discs were removed and immersed in 12 mL of phosphate-buffered saline (PBS) solution for 30 min. Afterward, 10 μL of liquid was extracted from each disc's PBS solution and again evenly spread across a new agar plate. This was followed by an incubation period of 18–24 h at a temperature of 37 ± 1 °C. Finally, the solution was subsequently diluted in PBS buffer, and 10 μL of these sample solutions was transferred onto Muller–Hinton agar (MHA) plates. The bacterial colonies on the MHA plates were counted after overnight incubation at 37 °C.

To conduct the long-time contact antibacterial experiment, another set of discs was incubated on bacteria-spread agar plates for 24 h at 37 °C. Then, the discs were removed carefully and immersed in a 12 mL PBS solution for 30 min to form a uniform bacterial suspension. A 100 μL sample suspension was serially diluted across six gradients, ranging from 10 times to 1 million times. Ten microliter liquid of the original gradient and each dilution gradient was dropped onto the agar plates and incubated for 18–24 h at 37 °C. Finally, the number of bacterial colonies resulting from each droplet was counted for analysis.[48−50]

The formula of calculating antibacterial ability is

$$\text{antibacterial percentage} = \frac{X_{n1} \times n1 - Y_{n2} \times n2}{X_{n1} \times n1} \times 100\%$$

where X_{n1} is the number of bacterial colonies incubated from the bacterial suspension that immerses the PLLA membrane and is diluted $n1$ times, $n1$ is the dilution time of the bacteria suspension that immerses PLLA membranes, Y_{n2} is the number of bacterial colonies incubated from the bacterial suspension that immerses the PLLA/Cu membrane and is diluted $n2$ times, and $n2$ is the dilution time of the bacterial suspension that immerses PLLA/Cu membranes.

3. RESULTS AND DISCUSSION

3.1. Surface Morphology. Electrospun PLLA fibers were treated with acetone to obtain the hierarchically porous fibers that have very high surface area. SEM pictures of the PLLA surfaces are shown in Figure 4a–f. Common electrospun PLLA fibers in previous research have solid fiber surfaces bearing only a few small pores. These pores mostly result from the phase separation that occurs between the nonsolvent and PLLA,[43] as shown in Figure S2. Note that these pores hardly span throughout the entire fibers. Hence, the surface area of common PLLA membranes is relatively small and must be

https://doi.org/10.1021/acsapm.3c03055
ACS Appl. Polym. Mater. 2024, 6, 2381−2391

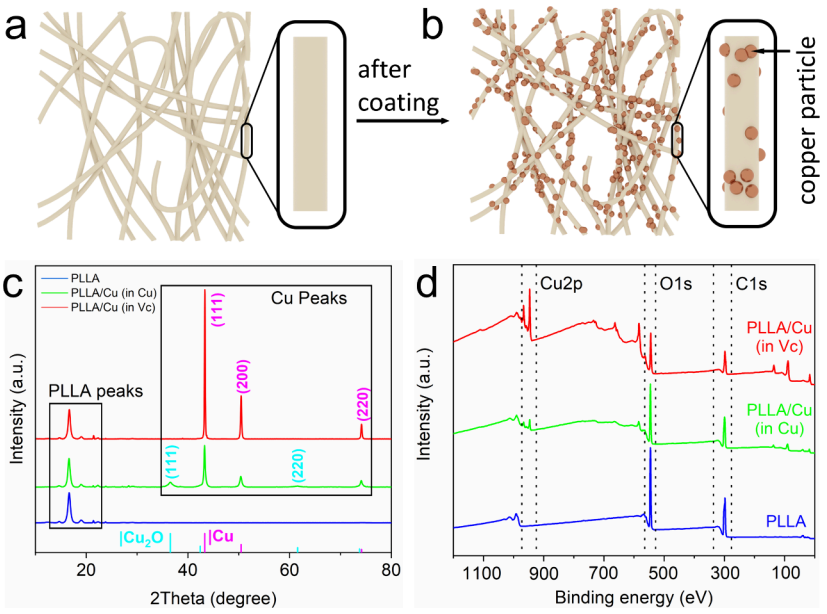

Figure 5. (a, b) Mechanisms of Cu particle coating. (c) XRD results. (d) XPS results.

further increased. In contrast, hierarchically porous PLLA fibers developed in this research contain a uniform, interpenetrating nanoporous network throughout, as well as an ultrarough surface (Figure 4a–d). The formation of these pores can be attributed to the acetone-induced recrystallization of PLLA.[42]

This kind of hierarchically porous structure significantly improves the fibrous specific surface area and pore density. With high specific surface area and high pore volume, more small particles, such as bacteria, can be captured. Moreover, the diffusion mechanism became more effective. Additionally, the fibers feature numerous nanopores, ranging in size from 10 to 100 nm, which can serve as traps to capture fine aerosol particles, such as PM2.5 and PM10.[52] Furthermore, due to the ultrahigh surface roughness of the hierarchically porous PLLA fibrous membrane, there is a higher friction coefficient between the fibers and the bacteria during air filtration. This could provide the membrane with more opportunities for interception. After acetone treatment, the PLLA membrane has a more stable general structure, as there is physical cross-linking between different fibers. Compared to the PLLA membrane before acetone treatment, the PLLA membrane after acetone treatment maintains a stable overall structure rather than collapsing during and after copper particle coating (Figure S3).

The SEM images of PLLA/Cu (in Cu) and PLLA/Cu (in Vc) are shown in Figure 4b,e and Figure 4c,f, respectively. After the coating procedure, copper particles were deposited on the surface of the PLLA fibers. The coating mechanism is shown in Figure 5a,b. It was observed that the nanofibers retained their original structure after Cu coating, confirming that the chemical reaction occurred without compromising the fiber structure. In general, the average diameter of copper particles on PLLA/Cu (in Cu) is smaller than that of PLLA/Cu (in Vc). The copper particles on PLLA/Cu (in Cu) have mainly submicrometer size (100 nm to 1 μm), while the majority of copper microparticles on PLLA/Cu (in Vc) fall within microsize (0.5 to 2 μm).

The size difference of copper particles can be attributed to the different ratios between the copper and ascorbic acid during the reaction, contributing to the different generation speeds of copper particles. As shown in Figure 3c, when the ascorbic acid solution is added into the copper solution, a larger amount of copper reacts with a smaller amount of ascorbic acid. Meanwhile, because the molar concentration of ascorbic acid is higher than that of copper, the copper ions are gradually reduced as the ascorbic acid solution disperses within the copper solution, resulting in smaller generated copper particles. Conversely, when the copper solution is added to the ascorbic acid solution, the opposite happens: the introduced copper ions are quickly reduced to elemental copper, leading to the formation of larger copper particles.

EDX results further confirm the copper deposition on the surface of samples. Figure S5 displays the copper EDX map images for PLLA/Cu (in Cu) and PLLA/Cu (in Vc). Figure S6 shows the ratio of the copper element detected by EDX. Notably, the copper wt % of PLLA/Cu (in Cu) is significantly less than that of PLLA/Cu (in Vc).

XRD patterns are shown in Figure 5c below. Untreated electrospun PLLA fibrous membranes exhibit lower crystallinity, manifested as a broad diffraction peak at around 16.5°. This is mainly due to the rapid evaporation of the solvent during the electrospinning process.[53] However, after acetone treatment, PLLA samples display four distinct peaks located at 14.7°, 16.5°, 19.0°, and 22.3°. These peaks primarily correspond to (010), (110)/(200), (203), and (015) planes, respectively.[43] This result indicates that the crystallinity of the electrospun PLLA fibers increased dramatically after acetone post-treatment.

In comparison to PLLA, both PLLA/Cu (in Cu) and PLLA/Cu (in Vc) show three additional distinct peaks located at 43.4°, 49.5°, and 73.3°. These peaks are attributed to the cooper particles and correspond to (111), (200), and (220) planes, respectively.[54] In addition, the XRD result also reveals that a greater amount of copper is present in PLLA/Cu (in Vc) than in PLLA/Cu (in Cu), consistent with the TGA data.

XPS examination was utilized to identify changes in the surface chemical composition after coating with Cu particles. As shown in the XPS surveys in Figure 5d, for pure PLLA

https://doi.org/10.1021/acsapm.3c03055
ACS Appl. Polym. Mater. 2024, 6, 2381−2391

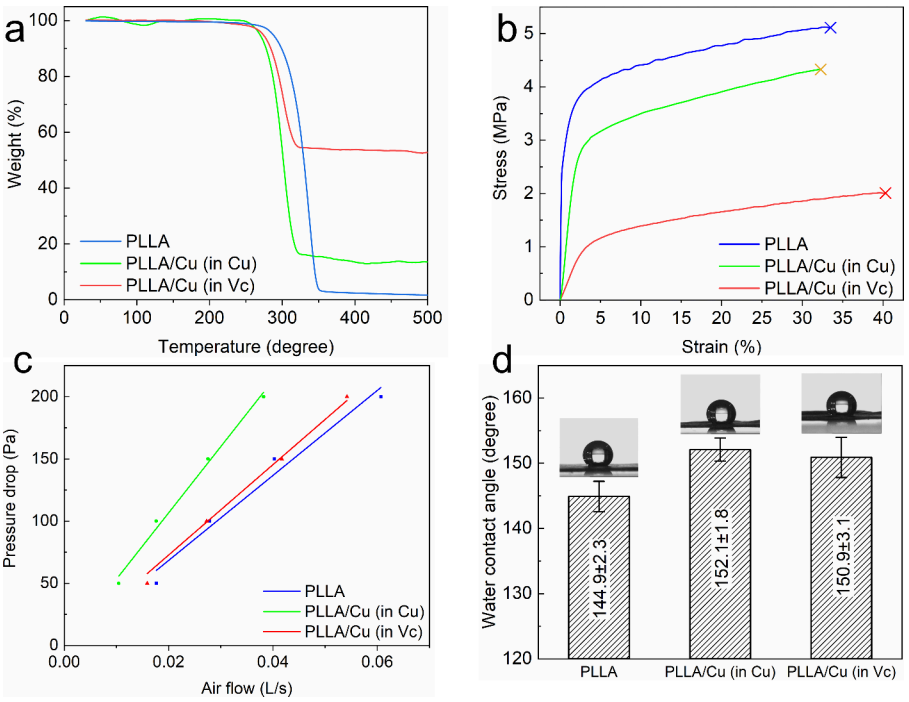

Figure 6. (a) TGA results of PLLA, PLLA/Cu (in Cu), and PLLA/Cu (in Vc). (b) Tensile strength results of PLLA, PLLA/Cu (in Cu), and PLLA/Cu (in Vc). (c) Air permeability results of PLLA, PLLA/Cu (in Cu), and PLLA/Cu (in Vc). (d) Water contact angle results of PLLA, PLLA/Cu (in Cu), and PLLA/Cu (in Vc).

samples, only O 1s (around 532 eV) and C 1s (around 284 eV) peaks could be detected. That is because PLLA only contain C═O, C−O, and O−C−O bonds.[55] Moreover, after coating Cu particles onto the PLLA samples, two new peaks associated with Cu emerged, which were located at around 933 and 952 eV. These two peaks correspond to the Cu 2p3/2 and Cu 2p1/2 transitions, respectively.[56] Additionally, much stronger Cu 2p3/2 and Cu 2p1/2a peaks were observed in the PLLA/Cu (in Vc) samples, indicating that a greater quantity of Cu particles was present on the surface of the PLLA/Cu (in Vc) samples.

3.2. Material Properties. TGA results of PLLA, PLLA/Cu (in Cu), and PLLA/Cu (in Vc) are shown in Figure 6a. For PLLA, decomposition begins at about 290 °C, reaching a maximum weight loss rate at around 350 °C. These thermal decomposition characteristics of PLLA align well with values reported in previous research.[57] In case of the PLLA/Cu (in Cu) and PLLA/Cu (in Vc) samples, the contents of Cu nano/microparticles can be estimated based on the residual amounts, as shown by the TGA measurements.[58] The results indicate that the copper particles comprise around 10% of the weight in PLLA/Cu (in Cu) and around 50% in PLLA/Cu (in Vc).

It is observed that the weight begins to decrease at lower temperature as the content of Cu particles increases. This behavior is likely due to copper's catalytic effect, which converts ester groups to hydroxyl groups in PLLA. As a result of this catalytic reaction, the average molecular mass decreases, making the substance more prone to vaporization.[59]

The reason for the higher weight percentage of copper in PLLA/Cu (in Vc) than in PLLA/Cu (in Cu) is the generating speed of copper particles. The concentration of the Vc solution is five times higher than that of the copper acetate solution. The molar mass of L-ascorbic acid is 176 g/mol, and the molar mass of copper acetate monohydrate is 199 g/mol. Therefore, the ratio of the Vc quantity and copper acetate quantity in the same solution volume is around 5.5:1. The high concentration of Vc allows a smaller volume of Vc to reduce a larger volume of copper acetate solution. Therefore, as shown in Figure 3c, when adding the Vc solution to the copper acetate solution, copper acetate is rapidly reduced to copper before all Vc solution is added. Conversely, when the copper acetate solution is added into the Vc solution, the reduction time equals the total time required for adding the copper acetate solution, allowing the PLLA membrane more time to capture the copper particles before they sink to the bottom. This results in higher copper weight percentage in PLLA/Cu (in Vc).

The mechanical strengths of PLLA, PLLA/Cu (in Cu), and PLLA/Cu (in Vc) are shown in Figure 6b. Compared to the untreated electrospun PLLA fibrous membrane, the hierarchically porous PLLA fibrous membrane exhibits a lower elongation at the break value (33.2%) but higher Young's modulus (0.12 GPa) and tensile strength (5.2 MPa). This is attributed to the ductile fracture behavior of the untreated electrospun PLLA fibrous membrane, which is predominantly amorphous. After undergoing acetone post-treatment, the membrane recrystallizes, enhancing its mechanical properties.[42,43]

PLLA/Cu (in Cu) and PLLA/Cu (in Vc) exhibit a similar elongation at the break value to those of PLLA (32.2 and 40.35%, respectively). However, both the tensile strength and Young's modulus of these samples are inferior to those of PLLA. Specifically, the tensile strength values are 4.3 MPa for PLLA/Cu (in Cu) and 2.1 MPa for PLLA/Cu (in Vc), while the Young's moduli are 0.014 and 0.0036 GPa, respectively. The reduction in tensile strength and Young's modulus is likely due to the presence of L-ascorbic acid. Ascorbic acid accelerates the degradation of the polymer, particularly for the polymer with higher molecular weight.[60] Given that PLLA/Cu (in Vc) was immersed in a Vc solution for an extended

https://doi.org/10.1021/acsapm.3c03055
ACS Appl. Polym. Mater. 2024, 6, 2381−2391

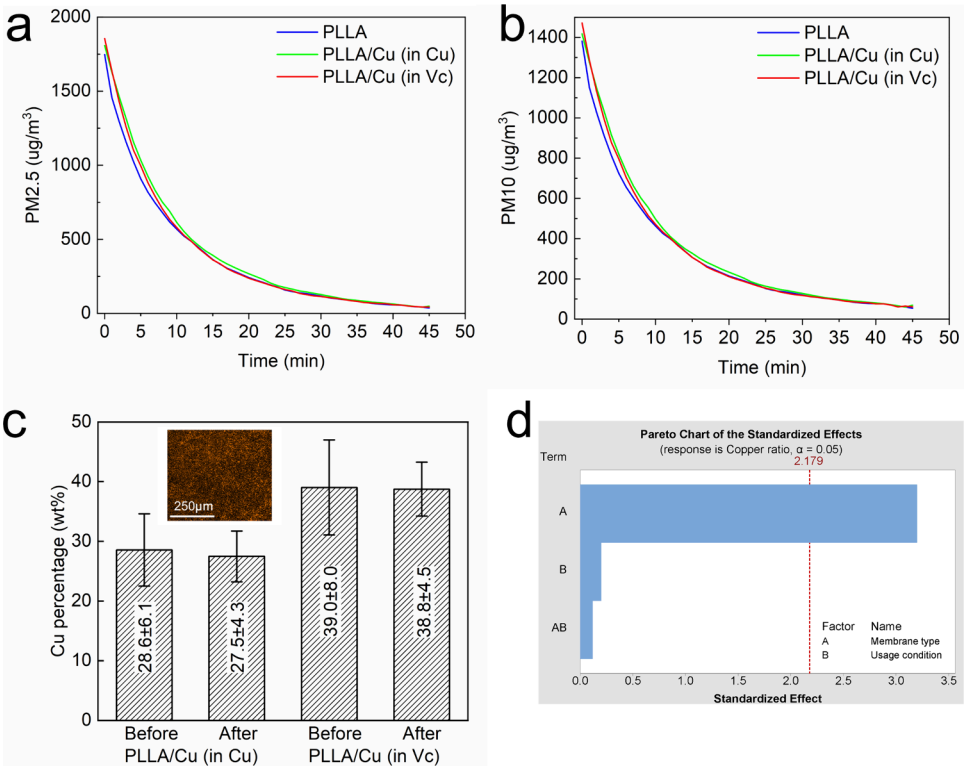

Figure 7. (a) PM2.5 filtration performance; (b) PM10 filtration performance; (c) percentage of the copper element detected by EDX map scanning. "Before" means the copper percentage detected on the sample before the air filtration testing, and "After" means the copper percentage after the testing. The size scanning area is shown within the graph. (d) Calculation result of Minitab.

period, it suffered from a more significant loss of mechanical strength.

Breathability is an important requirement for the air filtration membrane. The air permeabilities of PLLA/Cu (in Vc) and PLLA/Cu (in Cu) are illustrated in Figure 6c. Both sides of each type of sample were tested under various pressure settings, with each side tested once. The mean values from both sides were used to plot the fitted line. Compared to the PLLA samples, the air permeability of the coated samples slightly decreased as the air flow rate decreased under the same pressure drop. This suggests that coating the Cu particles on the PLLA fibrous membrane resulted in a higher pressure drop. This can be attributed to the added layers of Cu particles on the fibrous membrane. After the Cu particle coating, the basis weight of the fibrous membrane increased. Some void spaces were obstructed by the Cu particles, leading to a higher pressure drop due to less pores in the material.[61] Furthermore, the air permeability of the PLLA/Cu (in Cu) is significantly lower than that of PLLA/Cu (in Vc), indicating that PLLA/CU (in Cu) has smaller but more continuous small copper particles on its surface, which block more pores than on the PLLA/CU (in Vc) sample.

The wettability of the samples is shown in Figure 6d. Each type of sample was tested three times. It is widely recognized that PLLA is a hydrophobic material. Therefore, the water contact angle of PLLA samples in this research was 144.9 ± 2.3° as expected.[62] The deposition of copper particles onto the fibrous membrane made the surface rougher with higher contact angle.[63] Furthermore, copper particles could act as a nonwetting material, thereby increasing the hydrophobicity of the surface.[46] For these reasons, the contact angles of both kinds of PLLA/Cu exceeded 150°, completely transforming hydrophobic PLLA membranes into superhydrophobic PLLA/Cu fibrous membranes.

The flexibility of PLLA, PLLA/Cu (in Cu), and PLLA/Cu (in Vc) is shown in Figure S4. It is evident that both types of PLLA/Cu and PLLA possess excellent flexibility. Additionally, the color differences among the samples are notable: PLLA is white, PLLA/Cu (in Cu) is brown, and PLLA/Cu (in Vc) is pink.

3.3. Air Filtration Ability. To explore the air filtration capabilities, we established self-designed equipment based on commercial instruments. Figure 7a,b illustrates the filtration performance of PLLA, PLLA/Cu (in Cu), and PLLA/Cu (in Vc). The results show that all samples maintained similar filtration speeds, suggesting that the addition of the Cu particles did not adversely affect the air filtration ability of the hierarchically porous PLLA fibrous membrane.[43] With the filtration of all three kinds of membranes, the concentration of PM2.5 fell to less than 50 $\mu g/m^3$ from around 1700 $\mu g/m^3$ within 45 min, and PM10 fell to less than 100 $\mu g/m^3$ from around 1300 $\mu g/m^3$. All three kinds of membranes exhibit a good air filtration ability. Initially, the concentration of the particles was high, which resulted in a rapid decrease in the PM2.5 and PM10 concentrations. As these concentrations decreased, the rate of reduction also slowed down.

The ratios of the copper element detected by EDX are shown in Figure 7c, with four original spectra images presented in Figure S6. Each type of sample was tested four times. It is important to note that PLLA is sensitive to high-strength electron beams, so the beam intensity was reduced from 20 to 5 kV during high-magnification EDX mapping. Furthermore, the sizes of the copper particles on PLLA/Cu (in Cu) and PLLA/Cu (in Vc) were different. Their membrane surface was

https://doi.org/10.1021/acsapm.3c03055
ACS Appl. Polym. Mater. 2024, 6, 2381−2391

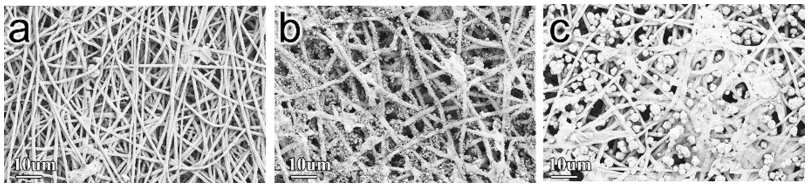

Figure 8. SEM image of (a) the PLLA fibrous membrane after filtration test, (b) PLLA/Cu (in Cu) fibrous membrane after filtration test, and (c) PLLA/Cu (in Vc) fibrous membrane after filtration test.

a

	Dilution level (1×10^n)	0	1	2	3	4	5	6
S. aureus	PLLA	N/C	N/C	N/C	N/C	N/C	N/C	I N/C
	PLLA/Cu (in Cu)	N/C	N/C	N/C	N/C	N/C	N/C	II 138
	PLLA/Cu (in Vc)	N/C	N/C	N/C	N/C	III 139	73	33
E. coli	PLLA	N/C	N/C	N/C	N/C	N/C	N/C	IV 38
	PLLA/Cu (in Cu)	N/C	N/C	N/C	V 20	3	1	1
	PLLA/Cu (in Vc)	VI 69	3	0	1	0	0	0

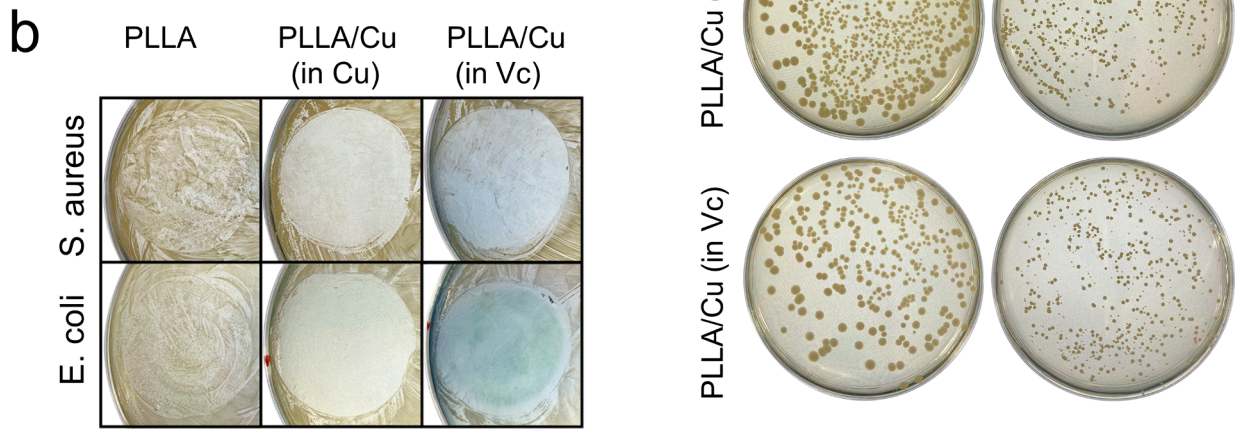

Figure 9. (a) Number of bacterial colonies grown from each solution drop in Figure S9. "N/C" means that the colony number is uncountable. (b) Areas where membrane samples were incubated with bacteria-spread agar plates after 24 h. (c) The agar plates were spread with bacterial suspensions and incubated overnight, with the method shown in Figure 3g–i.

porous and irregular, so the copper ratios were only useful for comparing changes in copper ratios on the membranes before and after filtration tests.

To validate whether the differences in copper ratios before and after filtration testing were not simple results of the testing process, Minitab was used to assess the correlation between copper ratio, membrane type, and usage condition. The data set included two factors: membrane type and usage condition. The membrane type included PLLA, PLLA/Cu (in Cu) and PLLA/Vc (in Vc). The usage condition was categorized as either "before testing" or "after testing". The four measurements of copper ratio for each membrane type and usage condition were input into software. The "Analyze Factorial Design" function within the Design of Experiments (DOE) was utilized. The results in Figure 7d and Figure S7 indicate that the differences of copper ratio are significantly influenced only by the membrane type rather than the usage condition.

The SEM images in Figure 8a–c reveal the general surface morphology of the fibrous membrane after air filtration experiments. The images demonstrate that oil stains from burnt Moxa were captured and visible on the surface of the membrane.[26] The outer surface of each individual fiber was covered with a layer of light, amorphous organic matter. As a result, the hierarchically porous structure became less distinct than that before filtration experiment, shown in Figure S8.

3.4. Antibacterial Performance. It is well known that incorporating metal or metal oxide particles into fiber composites enhances the antibacterial properties of the final composite materials.[64] Figure 9a and Figure S9 present the results of long-term antibacterial effectiveness of the various membrane samples. Roman numerals on Figure 9a target to the colonies of Figure S9. When tested against *S. aureus*, the antibacterial action of copper became evident from dilution level 4, as evidenced by the reduced number of bacterial colonies in the PLLA/Cu (in Cu) and PLLA/Cu (in Vc) groups compared to that in the PLLA group (control). Meanwhile, copper appeared to be more effective against *E. coli* than against *S. aureus*. When the membranes were incubated with *E. coli*, the bacterial colonies in the PLLA/Cu (in Cu) sample were fewer than those in PLLA starting at dilution level

https://doi.org/10.1021/acsapm.3c03055
ACS Appl. Polym. Mater. 2024, 6, 2381−2391

3. For the PLLA/Cu (in Vc) sample, *E. coli* colonies were even countable at dilution level 0. Based on the counting result of Figure 9a, the antibacterial effectiveness of PLLA/Cu (in Cu) against *S. aureus*, as calculated using the formula above, was 90%. The antibacterial effectiveness of PLLA/Cu (in Vc) against *S. aureus* was 99.9%. When it came to *E. coli*, the antibacterial effectiveness of PLLA/Cu (in Cu) was 99.9%, while that of PLLA/Cu (in Vc) reached an impressive 99.999%.

For the antibacterial efficacy of membranes under short time contact, shown in Figure 9c, both PLLA/Cu (in Cu) and PLLA/Cu (in Vc) significantly reduced the number of colonies for both *E. coli* and *S. aureus* within 1 min of contact. The disinfecting effects of two types of PLLA/Cu membranes appeared to be quite similar. The results strongly suggest that PLLA/Cu (in Vc) exhibits excellent antibacterial performance even within a brief contact time.

Figure 9b shows the areas where the samples were placed and incubated. After the removal of the PLLA discs, it was clearly observed that the bacteria grew only under the PLLA samples and not under the PLLA/Cu (in Cu) or PLLA/Cu (in Vc) samples. Additionally, the area under and near PLLA/Cu (in Vc) turned blue. Blue is the typical color of Cu^{2+}, indicating that during the experiment, the copper crystals on the PLLA/Cu (in Vc) sample became oxidated to copper ions[65] and spread onto the agar surface. In comparison, the blue color under or near the PLLA/Cu (in Cu) sample was less visible.

Compared to Gram-negative bacteria, the membrane of Gram-positive bacteria cannot be immediately depolarized by copper, which favored the survival rate of *S. aureus* in comparison to *E. coli* on PLLA/Cu membranes.[66] Since the antibacterial ability originates from copper, this explains why PLLA/Cu (in Vc) has better antibacterial properties than PLLA/Cu (in Cu). Moreover, Figure 9b demonstrates that PLLA/Cu (in Vc) releases more Cu^{2+} in comparison to PLLA/Cu (in Cu). A significant observation suggests that PLLA/Cu (in Vc) can kill bacteria more effectively. In addition to the impact of copper content, the difference in Cu^{2+} diffusivity between PLLA/Cu (in Cu) and PLLA/Cu (in Vc) could be influenced by the size of the copper particles.

In short, PLLA/Cu (in Vc) has better antibacterial ability and better air permeability than PLLA/Cu (in Cu) while still retaining reasonable tensile strength, similar bendability, superhydrophobic ability, and filtering quality.

4. CONCLUSIONS

To sum up, we have reported the preparation and characterizations of a group of hierarchically porous PLLA/Cu composite fibrous membranes with two methods and tested their air filtration and antibacterial abilities. The membrane coated with copper particles was prepared by using a simple immersing method. With a hierarchically porous structure, the prepared samples exhibited superhydrophobic properties with a water contact angle of over 150° after the deposition of copper nanoparticles. Electrospun polymer substrates and Cu particles were combined to empower the composite membranes with both good air filtration and antibacterial abilities. For the antibacterial ability, PLLA/Cu (in Vc) effectively kills more than 99.9% of *S. aureus* and more than 99.999% of *E. coli*. Furthermore, the results indicated that PLLA/Cu (in Vc) has better overall performance than PLLA/Cu (in Cu). Although the tensile strength of PLLA/Cu (in Vc) is inferior to that of PLLA/Cu (in Cu), it remains within an acceptable range. Therefore, the electrospun PLLA/Cu fibrous membrane developed in this work can be applied for the effective antibacterial filtration of various pollutants, including PM2.5 and PM10, as well as bacteria. This kind of membrane can be made through a simple and environmentally friendly process, and its antibacterial ability does not need extra environmental conditions, such as light and electricity. In view of its good air filtration capability in the closed environment and significant antibacterial ability, it is suitable to be used in the enclosed spaces that have biohazards, such as hospitals, nursing homes, and biology laboratories.

ASSOCIATED CONTENT

Supporting Information

The Supporting Information is available free of charge at https://pubs.acs.org/doi/10.1021/acsapm.3c03055.

Image of an air filtration testing machine; morphology of PLLA fibers before acetone treatment; images of the PLLA membranes after the copper coating procedure; bending ability of all samples; EDX maps and EDX spectra; analysis results from Minitab; high-magnification SEM images after air filtration test; optical pictures of agar plates after antibacterial test (PDF)

AUTHOR INFORMATION

Corresponding Authors

Jiashen Li − *Department of Materials, The University of Manchester, Manchester M13 9PL, U.K.*; orcid.org/0000-0001-7333-5280; Email: jiashen.li@manchester.ac.uk

Yi Li − *Department of Materials, The University of Manchester, Manchester M13 9PL, U.K.*; orcid.org/0000-0002-2092-4505; Email: henry.yili@manchester.ac.uk

Authors

Qinghong Huang − *Department of Materials, The University of Manchester, Manchester M13 9PL, U.K.*; orcid.org/0000-0003-0292-3717

Chen Meng − *Department of Materials, The University of Manchester, Manchester M13 9PL, U.K.*

Mingrui Liao − *Department of Physics & Astronomy, The University of Manchester, Manchester M13 9PL, U.K.*; orcid.org/0000-0002-9481-4026

Tianyu Kou − *Department of Materials, The University of Manchester, Manchester M13 9PL, U.K.*

Fangchao Zhou − *Faculty of Biology, Medicine and Health, The University of Manchester, Manchester M13 9PL, U.K.*

Jian R Lu − *Department of Physics & Astronomy, The University of Manchester, Manchester M13 9PL, U.K.*; orcid.org/0000-0001-5648-3564

Complete contact information is available at: https://pubs.acs.org/10.1021/acsapm.3c03055

Author Contributions

#C.M. and Q.H. make equal contributions to this research.

Notes

The authors declare no competing financial interest.

REFERENCES

(1) Gao, J.; Woodward, A.; Vardoulakis, S.; Kovats, S.; Wilkinson, P.; Li, L.; Xu, L.; Li, J.; Yang, J.; Li, J.; Cao, L.; Liu, X.; Wu, H.; Liu, Q. Haze, public health and mitigation measures in China: A review of the

current evidence for further policy response. *Sci. Total Environ.* **2017**, *578*, 148−157.
(2) Cheng, Z.; Cao, J.; Kang, L.; Luo, Y.; Li, T.; Liu, W. Novel transparent nano-pattern window screen for effective air filtration by electrospinning. *Mater. Lett.* **2018**, *221*, 157−160.
(3) Wan, H.; Wang, N.; Yang, J.; Si, Y.; Chen, K.; Ding, B.; Sun, G.; El-Newehy, M.; Al-Deyab, S. S.; Yu, J. Hierarchically structured polysulfone/titania fibrous membranes with enhanced air filtration performance. *J. Colloid Interface Sci.* **2014**, *417*, 18−26.
(4) Wang, Y.; Zhao, X.; Jiao, X.; Chen, D., Electrospun filters for air filtration: comparison with existing air filtration technologies. In *Filtering Media by Electrospinning: Next Generation Membranes for Separation Applications* 2018, 47−67 Springer, Cham DOI: 10.1007/978-3-319-78163-1_3.
(5) Kolkman, R. G. M.; Klaessens, J. H. M.; Hondebrink, E.; Hopman, J. C. W.; De Mul, F. F. M.; Steenbergen, W.; Thijssen, J. M.; Van Leeuwen, T. G. Photoacoustic determination of blood vessel diameter. *Phys. Med. Biol.* **2004**, *49* (20), 4745.
(6) Wang, N.; Zhu, Z.; Sheng, J.; Al-Deyab, S. S.; Yu, J.; Ding, B. Superamphiphobic nanofibrous membranes for effective filtration of fine particles. *J. Colloid Interface Sci.* **2014**, *428*, 41−48.
(7) Zhu, M.; Han, J.; Wang, F.; Shao, W.; Xiong, R.; Zhang, Q.; Pan, H.; Yang, Y.; Samal, S. K.; Zhang, F.; Huang, C. Electrospun nanofibers membranes for effective air filtration. *Macromol. Mater. Eng.* **2017**, *302* (1), No. 1600353.
(8) Chuanfang, Y. Aerosol filtration application using fibrous media—an industrial perspective. *Chin. J. Chem. Eng.* **2012**, *20* (1), 1−9.
(9) Ge, T.; Hu, X.; Liao, M.; Zhou, F.; Lu, J. R. Recent Advances in the Development and Application of Peptide Self-Assemblies in Infection Control. *Curr. Opin. Colloid Interface Sci.* **2023**, *68*, No. 101745.
(10) Khalid, B.; Bai, X.; Wei, H.; Huang, Y.; Wu, H.; Cui, Y. Direct blow-spinning of nanofibers on a window screen for highly efficient PM2. 5 removal. *Nano Lett.* **2017**, *17* (2), 1140−1148.
(11) Liu, C.; Hsu, P.-C.; Lee, H.-W.; Ye, M.; Zheng, G.; Liu, N.; Li, W.; Cui, Y. Transparent air filter for high-efficiency PM2. 5 capture. *Nat. Commun.* **2015**, *6* (1), 6205.
(12) Ciorîţă, A.; Suciu, M.; Coroş, M.; Varodi, C.; Pogăcean, F.; Măgeruşan, L.; Mirel, V.; Staden, R.-I. Ş.-V.; Pruneanu, S. Antibacterial Enhancement of High-Efficiency Particulate Air Filters Modified with Graphene-Silver Hybrid Material. *Microorganisms* **2023**, *11* (3), 745.
(13) Day, D.; Xiang, J.; Mo, J.; Clyde, M.; Weschler, C.; Li, F.; Gong, J.; Chung, M.; Zhang, Y.; Zhang, J. Combined use of an electrostatic precipitator and a high-efficiency particulate air filter in building ventilation systems: Effects on cardiorespiratory health indicators in healthy adults. *Indoor air* **2018**, *28* (3), 360−372.
(14) Mead, K.; Johnson, D. L. An evaluation of portable high-efficiency particulate air filtration for expedient patient isolation in epidemic and emergency response. *Annals of emergency medicine* **2004**, *44* (6), 635−645.
(15) Perry, J. L.; Agui, J.; Vijayakimar, R. *Submicron and nanoparticulate matter removal by HEPA-rated media filters and packed beds of granular materials*; 2016 NASA Marshall Space Flight Center.
(16) Christopherson, D. A.; Yao, W. C.; Lu, M.; Vijayakumar, R.; Sedaghat, A. R. High-efficiency particulate air filters in the era of COVID-19: function and efficacy. *Otolaryngol.−Head Neck Surg.* **2020**, *163* (6), 1153−1155.
(17) Liu, H.; Huang, J.; Mao, J.; Chen, Z.; Chen, G.; Lai, Y. Transparent antibacterial nanofiber air filters with highly efficient moisture resistance for sustainable particulate matter capture. *Iscience* **2019**, *19*, 214−223.
(18) Gao, Y.; Tian, E.; Zhang, Y.; Mo, J. Utilizing electrostatic effect in fibrous filters for efficient airborne particles removal: Principles, fabrication, and material properties. *Applied Materials Today* **2022**, *26*, No. 101369.
(19) Li, P.; Wang, C.; Zhang, Y.; Wei, F. Air filtration in the free molecular flow regime: a review of high-efficiency particulate air filters based on carbon nanotubes. *Small* **2014**, *10* (22), 4543−4561.
(20) Lu, T.; Cui, J.; Qu, Q.; Wang, Y.; Zhang, J.; Xiong, R.; Ma, W.; Huang, C. Multistructured electrospun nanofibers for air filtration: a review. *ACS Appl. Mater. Interfaces* **2021**, *13* (20), 23293−23313.
(21) Henning, L. M.; Abdullayev, A.; Vakifahmetoglu, C.; Simon, U.; Bensalah, H.; Gurlo, A.; Bekheet, M. F. Review on polymeric, inorganic, and composite materials for air filters: from processing to properties. *Adv. Energy Sustainability Res.* **2021**, *2* (5), No. 2100005.
(22) Xu, J.; Liu, C.; Hsu, P.-C.; Liu, K.; Zhang, R.; Liu, Y.; Cui, Y. Roll-to-roll transfer of electrospun nanofiber film for high-efficiency transparent air filter. *Nano Lett.* **2016**, *16* (2), 1270−1275.
(23) Zhang, R.; Liu, C.; Hsu, P. C.; Zhang, C.; Liu, N.; Zhang, J.; Lee, H. R.; Lu, Y.; Qiu, Y.; Chu, S.; Cui, Y. Nanofiber air filters with high-temperature stability for efficient PM2. 5 removal from the pollution sources. *Nano Lett.* **2016**, *16* (6), 3642−3649.
(24) Wang, Q.; Bai, Y.; Xie, J.; Jiang, Q.; Qiu, Y. Synthesis and filtration properties of polyimide nanofiber membrane/carbon woven fabric sandwiched hot gas filters for removal of PM 2.5 particles. *Powder Technol.* **2016**, *292*, 54−63.
(25) Wang, F.; Dai, J.; Huang, L.; Si, Y.; Yu, J.; Ding, B. Biomimetic and superelastic silica nanofibrous aerogels with rechargeable bactericidal function for antifouling water disinfection. *ACS Nano* **2020**, *14* (7), 8975−8984.
(26) Song, J.; Zhao, Q.; Meng, C.; Meng, J.; Chen, Z.; Li, J. Hierarchical Porous Recycled PET Nanofibers for High-Efficiency Aerosols and Virus Capturing. *ACS Appl. Mater. Interfaces* **2021**, *13* (41), 49380−49389.
(27) Yin, N.; Zhuge, Y.; Ji, H.; Liu, F. *Effective preparation of environmentally friendly polyglycolic acid (PGA) nanofibrous membrane with antibacterial property for high-efficiency and low-resistance air filtration* Research Square Platform LLC. 2023 DOI: 10.21203/rs.3.rs-2651786/v1.
(28) Liu, Y.; Liang, X.; Wang, S.; Qin, W.; Zhang, Q. Electrospun antimicrobial polylactic acid/tea polyphenol nanofibers for food-packaging applications. *Polymers* **2018**, *10* (5), 561.
(29) Sawai, J. Quantitative evaluation of antibacterial activities of metallic oxide powders (ZnO, MgO and CaO) by conductimetric assay. *J. Microbiol. Methods* **2003**, *54* (2), 177−182.
(30) Suryaprabha, T.; Sethuraman, M. G. Fabrication of copper-based superhydrophobic self-cleaning antibacterial coating over cotton fabric. *Cellulose* **2017**, *24*, 395−407.
(31) Cimini, A.; Borgioni, A.; Passarini, E.; Mancini, C.; Proietti, A.; Buccini, L.; Stornelli, E.; Schifano, E.; Dinarelli, S.; Mura, F.; Sergi, C.; Bavasso, I.; Cortese, B.; Passeri, D.; Imperi, E.; Rinaldi, T.; Picano, A.; Rossi, M. Upscaling of Electrospinning Technology and the Application of Functionalized PVDF-HFP@ TiO2 Electrospun Nanofibers for the Rapid Photocatalytic Deactivation of Bacteria on Advanced Face Masks. *Polymers* **2023**, *15* (23), 4586.
(32) Choi, D. Y.; Heo, K. J.; Kang, J.; An, E. J.; Jung, S.-H.; Lee, B. U.; Lee, H. M.; Jung, J. H. Washable antimicrobial polyester/aluminum air filter with a high capture efficiency and low pressure drop. *Journal of hazardous materials* **2018**, *351*, 29−37.
(33) Karthick, S. A.; Gobi, N. Nano silver incorporated electrospun polyacrylonitrile nanofibers and spun bonded polypropylene composite for aerosol filtration. *Journal of Industrial Textiles* **2017**, *46* (6), 1342−1361.
(34) Lanone, S.; Rogerieux, F.; Geys, J.; Dupont, A.; Maillot-Marechal, E.; Boczkowski, J.; Lacroix, G.; Hoet, P. Comparative toxicity of 24 manufactured nanoparticles in human alveolar epithelial and macrophage cell lines. *Part. Fibre Toxicol.* **2009**, *6* (1), 1−12.
(35) Slavin, Y. N.; Asnis, J.; Häfeli, U. O.; Bach, H. Metal nanoparticles: understanding the mechanisms behind antibacterial activity. *J. Nanobiotechnol.* **2017**, *15*, 1−20.
(36) Santo, C. E.; Taudte, N.; Nies, D. H.; Grass, G. Contribution of copper ion resistance to survival of Escherichia coli on metallic copper surfaces. *Applied and environmental microbiology* **2008**, *74* (4), 977−986.

(37) Misra, S. K.; Dybowska, A.; Berhanu, D.; Luoma, S. N.; Valsami-Jones, E. The complexity of nanoparticle dissolution and its importance in nanotoxicological studies. *Science of the total environment* **2012**, *438*, 225−232.
(38) Gunawan, C.; Teoh, W. Y.; Marquis, C. P.; Amal, R. Cytotoxic origin of copper (II) oxide nanoparticles: comparative studies with micron-sized particles, leachate, and metal salts. *ACS Nano* **2011**, *5* (9), 7214−7225.
(39) Perelshtein, I.; Lipovsky, A.; Perkas, N.; Gedanken, A.; Moschini, E.; Mantecca, P. The influence of the crystalline nature of nano-metal oxides on their antibacterial and toxicity properties. *Nano Research* **2015**, *8*, 695−707.
(40) Ali, A.; Baheti, V.; Militky, J.; Khan, Z.; Tunakova, V.; Naeem, S. Copper coated multifunctional cotton fabrics. *Journal of Industrial Textiles* **2018**, *48* (2), 448−464.
(41) Zhu, M.; Cao, Q.; Liu, B.; Guo, H.; Wang, X.; Han, Y.; Sun, G.; Li, Y.; Zhou, J. A novel cellulose acetate/poly (ionic liquid) composite air filter. *Cellulose* **2020**, *27*, 3889−3902.
(42) Lu, Z.; Zhang, B.; Gong, H.; Li, J. Fabrication of hierarchical porous poly (l-lactide)(PLLA) fibrous membrane by electrospinning. *Polymer* **2021**, *226*, No. 123797.
(43) Song, J.; Zhang, B.; Lu, Z.; Xin, Z.; Liu, T.; Wei, W.; Zia, Q.; Pan, K.; Gong, R. H.; Bian, L.; Li, Y.; Li, J. Hierarchical porous poly (l-lactic acid) nanofibrous membrane for ultrafine particulate aerosol filtration. *ACS Appl. Mater. Interfaces* **2019**, *11* (49), 46261−46268.
(44) Chang, J.; Meng, C.; Shi, B.; Wei, W.; Li, R.; Meng, J.; Wen, H.; Wang, X.; Song, J.; Hu, Z.; Liu, Z.; Li, J. Flexible, breathable, and reinforced ultra-thin Cu/PLLA porous-fibrous membranes for thermal management and electromagnetic interference shielding. *J. Mater. Sci. Technol.* **2023**, *161*, 150.
(45) Liu, Z.; Li, Z.; Zhai, H.; Jin, L.; Chen, K.; Yi, Y.; Gao, Y.; Xu, L.; Zheng, Y.; Yao, S.; Liu, Z.; Li, G.; Song, Q.; Yue, P.; Xie, S.; Li, Y.; Zheng, Z. A highly sensitive stretchable strain sensor based on multi-functionalized fabric for respiration monitoring and identification. *Chem. Eng. J.* **2021**, *426*, No. 130869.
(46) Rezaie, A. B.; Montazer, M.; Rad, M. M. Low toxic antibacterial application with hydrophobic properties on polyester through facile and clean fabrication of nano copper with fatty acid. *Mater. Sci. Eng.: C* **2019**, *97*, 177−187.
(47) Huang, X.; Jiao, T.; Liu, Q.; Zhang, L.; Zhou, J.; Li, B.; Peng, Q. Hierarchical electrospun nanofibers treated by solvent vapor annealing as air filtration mat for high-efficiency PM2. 5 capture. *Sci. China Mater.* **2019**, *62* (3), 423−436.
(48) Qian, J.; Dong, Q.; Chun, K.; Zhu, D.; Zhang, X.; Mao, Y.; Culver, J. N.; Tai, S.; German, J. R.; Dean, D. P.; Miller, J. T.; Wang, L.; Wu, T.; Li, T.; Brozena, A. H.; Briber, R. M.; Milton, D. K.; Bentley, W. E.; Hu, L. Highly stable, antiviral, antibacterial cotton textiles via molecular engineering. *Nat. Nanotechnol.* **2023**, *18* (2), 168−176.
(49) Liao, M.; Gong, H.; Liu, H.; Shen, K.; Ge, T.; King, S.; Schweins, R.; McBain, A. J.; Hu, X.; Lu, J. R. Combination of a pH-responsive peptide amphiphile and a conventional antibiotic in treating Gram-negative bacteria. *J. Colloid Interface Sci.* **2023**, *659*, 397.
(50) Liao, M.; Gong, H.; Quan, X.; Wang, Z.; Hu, X.; Chen, Z.; Li, Z.; Liu, H.; Zhang, L.; McBain, A. J.; Waigh, T. A.; Zhou, J.; Lu, J. R. Intramembrane Nanoaggregates of Antimicrobial Peptides Play a Vital Role in Bacterial Killing. *Small* **2023**, *19* (3), No. 2204428.
(51) Andric, T.; Wright, L. D.; Taylor, B. L.; Freeman, J. W. Fabrication and characterization of three-dimensional electrospun scaffolds for bone tissue engineering. *J. Biomed. Mater. Res., Part A* **2012**, *100A* (8), 2097−2105.
(52) Vecchi, R.; Marcazzan, G.; Valli, G.; Ceriani, M.; Antoniazzi, C. The role of atmospheric dispersion in the seasonal variation of PM1 and PM2. 5 concentration and composition in the urban area of Milan (Italy). *Atmos. Environ.* **2004**, *38* (27), 4437−4446.
(53) Monticelli, O.; Bocchini, S.; Gardella, L.; Cavallo, D.; Cebe, P.; Germelli, G. Impact of synthetic talc on PLLA electrospun fibers. *European polymer journal* **2013**, *49* (9), 2572−2583.
(54) Rezaie, A. B.; Montazer, M. One-step fabrication of fatty acids/nano copper/polyester shape-stable composite phase change material for thermal energy management and storage. *Applied energy* **2018**, *228*, 1911−1920.
(55) Zia, Q.; Tabassum, M.; Meng, J.; Xin, Z.; Gong, H.; Li, J. Polydopamine-assisted grafting of chitosan on porous poly (L-lactic acid) electrospun membranes for adsorption of heavy metal ions. *Int. J. Biol. Macromol.* **2021**, *167*, 1479−1490.
(56) Dai, J.; Yang, H.; Yan, H.; Shangguan, Y.; Zheng, Q.; Cheng, R. Phosphate adsorption from aqueous solutions by disused adsorbents: chitosan hydrogel beads after the removal of copper (II). *Chemical Engineering Journal* **2011**, *166* (3), 970−977.
(57) Meng, C.; Tang, D.; Liu, X.; Meng, J.; Wei, W.; Gong, R. H.; Li, J. Heterogeneous porous PLLA/PCL fibrous scaffold for bone tissue regeneration. *Int. J. Biol. Macromol.* **2023**, *235*, No. 123781.
(58) Jia, B.; Mei, Y.; Cheng, L.; Zhou, J.; Zhang, L. Preparation of copper nanoparticles coated cellulose films with antibacterial properties through one-step reduction. *ACS Appl. Mater. Interfaces* **2012**, *4* (6), 2897−2902.
(59) Popescu, V.; Prodan, D.; Cuc, S.; Saroşi, C.; Furtos, G.; Moldovan, A.; Carpa, R.; Bomboş, D. Antimicrobial Poly (Lactic Acid)/Copper Nanocomposites for Food Packaging Materials. *Materials* **2023**, *16* (4), 1415.
(60) Vijayalakshmi, S.; Raichur, A.; Madras, G. Thermal degradation of poly (ethylene oxide) and polyacrylamide with ascorbic acid. *J. Appl. Polym. Sci.* **2006**, *101* (5), 3067−3072.
(61) Zhao, M.; Liao, L.; Xiao, W.; Yu, X.; Wang, H.; Wang, Q.; Lin, Y. L.; Kilinc-Balci, F. S.; Price, A.; Chu, L.; Chu, M. C.; Chu, S.; Cui, Y. Household materials selection for homemade cloth face coverings and their filtration efficiency enhancement with triboelectric charging. *Nano Lett.* **2020**, *20* (7), 5544−5552.
(62) Lu, Z.; Zia, Q.; Meng, J.; Liu, T.; Song, J.; Li, J. Hierarchical porous poly (l-lactic acid)/SiO2 nanoparticles fibrous membranes for oil/water separation. *J. Mater. Sci.* **2020**, *55* (34), 16096−16110.
(63) Cho, K.-H.; Chen, L.-J. Fabrication of sticky and slippery superhydrophobic surfaces via spin-coating silica nanoparticles onto flat/patterned substrates. *Nanotechnology* **2011**, *22* (44), No. 445706.
(64) Mihailović, D.; Šaponjić, Z.; Vodnik, V.; Potkonjak, B.; Jovančić, P.; Nedeljković, J. M.; Radetić, M. Multifunctional PES fabrics modified with colloidal Ag and TiO2 nanoparticles. *Polym. Adv. Technol.* **2011**, *22* (12), 2244−2249.
(65) Naga, N.; Yoshida, Y.; Inui, M.; Noguchi, K.; Murase, S. Crystallization of amorphous poly (lactic acid) induced by organic solvents. *J. Appl. Polym. Sci.* **2011**, *119* (4), 2058−2064.
(66) Warnes, S.; Keevil, C. Mechanism of copper surface toxicity in vancomycin-resistant enterococci following wet or dry surface contact. *Applied and environmental microbiology* **2011**, *77* (17), 6049−6059.

https://doi.org/10.1021/acsapm.3c03055
ACS Appl. Polym. Mater. 2024, 6, 2381−2391